Frequency-Preserved Acoustic Diode Model with High Forward-Power-Transmission Rate

Chang Liu,[1] Zongliang Du,[1] Zhi Sun,[1] Huajian Gao,[2] and Xu Guo[1,*]

[1]*State Key Laboratory of Structural Analysis for Industrial Equipment, Department of Engineering Mechanics, Dalian University of Technology, Dalian 116023, People's Republic of China*
[2]*School of Engineering, Brown University, Providence, Rhode Island 02912, USA*

The acoustic diode (AD) can provide brighter and clearer ultrasound images by eliminating acoustic disturbances caused by sound waves traveling in two directions at the same time and interfering with each other. Such an AD could give designers new flexibility in making ultrasonic sources like those used in medical imaging or nondestructive testing. However, current AD designs, based on nonlinear effects, only partially fill this role by converting sound to a new frequency and blocking any backward flow of the original frequency. In this work, an AD model that preserves the frequencies of acoustic waves and has a relatively high forward-power-transmission rate is proposed. Theoretical analysis indicates that the proposed AD has forward, reverse, and breakdown characteristics very similar to electrical diodes. The significant rectifying effect of the proposed AD is verified numerically through a one-dimensional example. Possible schemes for experimental realization of this model as well as more complex and efficient AD designs are also discussed.

I. INTRODUCTION

The invention of the electric diode, which realized the rectification of electric-current flux for the first time, marked the advent of modern electronics and eventually changed our daily lives significantly. Inspired by the remarkable energy-rectification characteristics of electric diodes, recent years have witnessed growing research interest in controlling other forms of energy flux in a similar manner [1–6]. Among these contributions, a lot of attempts have been made to design an acoustic diode (AD) that can rectify acoustic-energy flux. The acoustic diode is a device that allows acoustic or elastic waves to travel along one direction but not in the opposite direction. This one-way flow of sound would provide brighter and clearer ultrasound images by eliminating acoustic disturbances caused by sound waves going in two directions at the same time and interfering with each other. In practice, such an AD could give designers new flexibility in making ultrasonic sources like those used in medical imaging or nondestructive testing [7,8]. This kind of device also promises to be of great benefit for shock-wave lithotripsy [9], vibration mitigation, environmental noise control [10], and could even be used as a building block in acoustic-elastic logic gates, in analogy to electronics [11,12].

The first theoretical model of an AD was presented by Cheng and coworkers in 2009 [7], and then various AD models that can achieve asymmetrical transmission of acoustic waves were suggested [12–17]. It is worth noting,

however, that all proposed ADs based on linear structures should not be identified as diodes in a strict sense because the reciprocity principle of linear systems must be respected [18]. The ADs based on the nonlinear effect all need to change the frequencies of acoustic waves. Due to the poor conversion efficiency in nonlinear systems, only a small part of wave energy can pass through the systems. Therefore, the forward-power-transmission rates of these ADs are relatively low. A major challenge yet to be tackled is how to utilize nonlinear effects to achieve acoustic-wave rectification in a perfectly asymmetric fashion without changing the direction and frequency of the incident wave and, at the same time, maintaining higher forward-power-transmission rates [18]. It is worth noting that a strictly nonreciprocal acoustic circulator (not an AD) with high forward transmission without using nonlinear effects was proposed in Ref [19]. The scheme in that article seems another promising way to design effective ADs.

In this work, a different theoretical model is proposed for ADs. Compared with other ADs based on nonlinear effects [7,8,12], the distinctive feature of the proposed model is such that one-way energy transmission can be achieved without changing the frequencies of the incident waves. Because of the weak nonlinearity, most of wave energy can be kept in the original frequency. So, theoretically, if the impedance of the interfaces can be designed appropriately, a perfect acoustic isolator [18] can be realized, for which the corresponding power-transmission rate R_T is almost unity (i.e., $R_T \approx 1$) in one direction and $R_T \approx 0$ in the opposite direction. Possible schemes for experimental realization of this model, as well as more complex and efficient acoustic diode designs, are also discussed in this paper.

[*]To whom correspondence should be addressed.
guoxu@dlut.edu.cn

II. THEORETICAL MODEL

One of the key points for designing the present AD model is resorting to the nonlinear periodic systems (e.g., a nonlinear phononic crystal) that can provide amplitude-dependent band structures [20], in order to break the restriction of the reciprocal theorem in linear acoustic systems. Since amplitude-dependent dispersion is only a weak nonlinear effect in this wave propagation system, the energy associated with the excited higher-frequency harmonic waves can be ignored [21], which may ensure the high forward-power-transmission rate. Asymmetric linear structures are then introduced to modulate the wave amplitudes in an incident direction-dependent way. This constitutes the other cornerstone of the present AD model.

Figure 1 illustrates schematically a prototype of the proposed AD model. A harmonic force acts on the left side of the AD device, If the amplitude and the frequency of the incident wave [i.e., (ω, A)] are located in the passband of the weakly nonlinear phononic crystal, whose dispersion property is wave-amplitude dependent, then the harmonic wave can pass through the filter nearly lossless. However, due to the asymmetry deliberately introduced into the system, if the same harmonic excitation acts on the right side of the AD device, the amplitude of the incident wave may be modulated to A' and (ω, A') may locate in the forbidden band of the nonlinear phononic crystal. Under these circumstances, the wave coming from the right side cannot pass through the system and the system can be reasonably referred to as an AD.
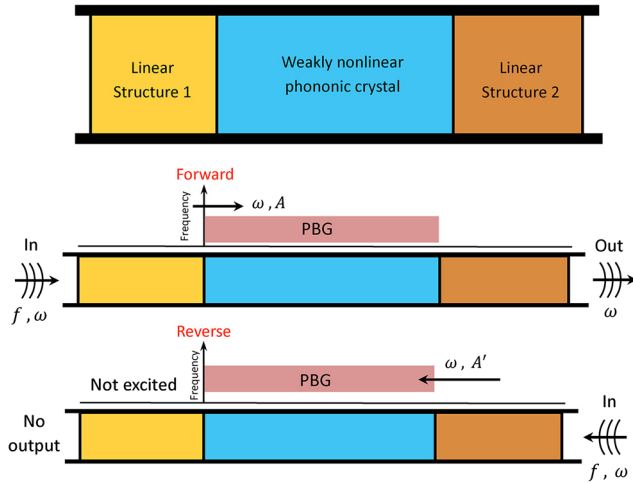

FIG. 1. Schematic illustration of the AD model. When the harmonic force with amplitude f and frequency ω acts on the left side, the wave incident on the nonlinear periodic structure is outside the passband gap (PBG) and can pass through the system. While the same force acts on the other side, the wave cannot pass through the system.

III. NUMERICAL EXPERIMENT

A. A one-dimensional, semidiscrete example

Although the aforementioned principle can be applied to designing ADs in any spatial dimension, here a fairly simple, one-dimensional example is chosen to verify the effectiveness of the proposed AD model. As shown in Fig. 2(a), a one-dimensional AD is constructed of a number of rigid balls connected by linear and weakly nonlinear springs. The asymmetry of the system is introduced by one, uniform cross-section, linear elastic rod and another linear elastic rod with variable cross sectional area at two ends of the mass chain. When an acoustic wave propagates through the nonuniform rod, its amplitude is changed because of the energy-conservation principle. Furthermore, the magnifying coefficient can be controlled by appropriately selecting the structural parameters of the rod.

Assume that the force-elongation relationship of the weakly nonlinear spring [the yellow spring in Fig. 2(a)] is $f = \alpha k \delta + \Gamma \delta^3$, where δ denotes the elongation of the nonlinear spring and αk $(\alpha > 0)$ and $\Gamma > 0$ are the stiffness parameters of the spring $(\Gamma \delta^2 / \alpha k \ll 1)$. Here, the symbol k is the stiffness coefficient of the linear spring [the blue spring in Fig. 2(a)]. With use of the perturbation approach [20], it can be found that the dispersion relationship of the weakly nonlinear mass-spring system is

$$\bar{\omega} \approx \sqrt{2 + \alpha - 2\cos(p)} + \frac{3}{8}\frac{\Gamma d^2}{k}\frac{|\bar{A}_0|^2}{\sqrt{2 + \alpha - 2\cos(p)}}, \quad (1)$$

where $\bar{\omega} = \omega/\omega_0$, with $\omega_0 = \sqrt{k/m}$ denoting the nondimensional frequency, and d and m are the length of the unit cell and the mass of the ball, respectively. In Eq. (1), $p = hd$ is the nondimensional Bloch wave number with h denoting the usual Bloch wave number and $\bar{A}_0 = A_0/d$ is the nondimensional amplitude of the incident wave.

Figure 2(b) depicts the dispersion relationship predicted by the perturbation analysis with different wave amplitudes. Figure 2(c) presents a closer view of the dispersion behavior near the upper cutoff frequency. It can be seen that the mass-spring system has only one passband, and that the lower and the upper bound of the passband increase when the amplitude of the incident wave is increased. This indicates that, when the incident-wave frequency falls into the range of $2.236\omega_0$–$2.253\omega_0$ [the orange shaded area in Fig. 2(c)], only when $|\bar{A}_0|^2 > a_\omega$ (a_ω is a function of ω, and $a_\omega > 0.001$), then the incident wave can propagate through the nonlinear mass-spring chain. However, when $|\bar{A}_0|^2 < a_\omega$, the wave will undergo exponential attenuations as it propagates. Therefore, for a specific range of frequencies, the nonlinear mass-spring chain can serve as an amplitude-dependent wave filter. This property plays a crucial role in the current AD model.

As shown in Fig. 2(a), the asymmetry wave amplitude modulation can be achieved by placing an elastic rod r_1
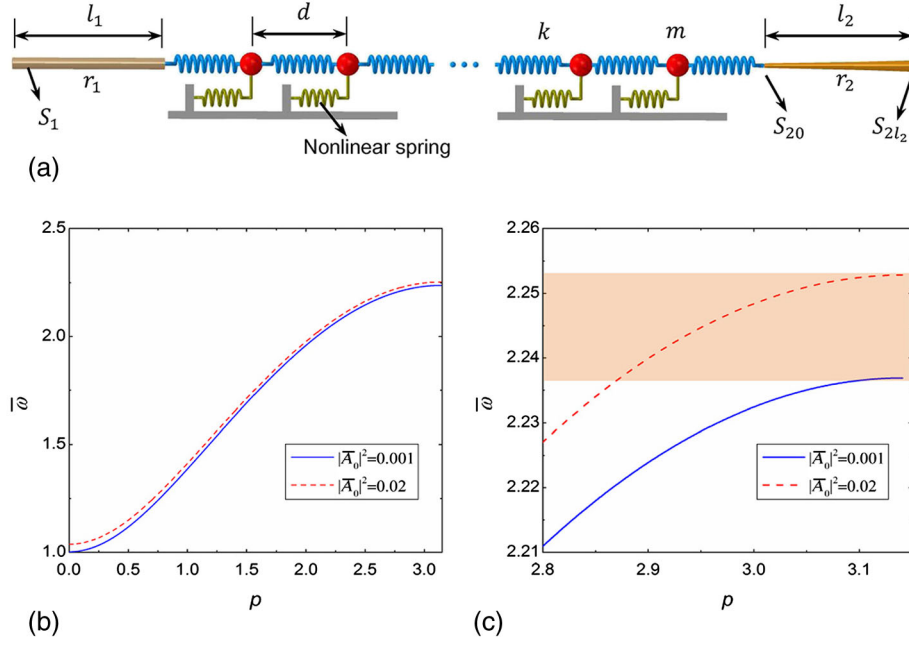
FIG. 2. (a) A simple, one-dimensional example of the AD model in this work. (b) The dispersion relationship of the nonlinear periodic chain with different wave amplitudes. Here $\alpha = 1$, $\Gamma d^2/k = 5$. (c) A closer view of the dispersion behavior near the upper cutoff frequency.

with uniform cross-sectional area at the left side of the nonlinear mass-spring chain, while placing an elastic rod r_2 with nonuniform cross-sectional area at the other side. Actually, when the area of the rod varies along its length and is in the form of $S(x) = S_0 \exp[\ln(S_l/S_0)x/l]$ (here, S_0 and S_l are the small-end area and the big-end area, respectively, and l denotes the length of the rod), the corresponding magnifying coefficient (i.e., the ratio of the displacements at $x = 0$ and $x = l$) can be obtained as

$$M = \frac{\sqrt{S_0/S_l}\,\mathrm{Re}(Ae^{-iql} + Be^{iql})}{\mathrm{Re}(A + B)}, \qquad (2)$$

where $q = \sqrt{(\omega^2/c^2) - (\chi^2/4)}$ and $\chi = (1/l)\ln(S_0/S_l)$. For the rod with uniform cross-sectional area, we have $\chi = 0$. In Eq. (2), ω is the frequency of the incident wave, $c = \sqrt{E/\rho}$ denotes the wave velocity (E and ρ are the Young's modulus and density of the rod material, respectively) and A and B represent the amplitude of the incident and the reflected wave in the rod, respectively.

B. Numerical method and parameters

The propagation of acoustic waves in this nonlinear system can be investigated numerically by using the Runge-Kutta algorithm. The rods at the two ends are discretized as two linear mass-spring chains through a lumped mass method. Then the driving forces are exerted on the mass located at the edge of the discretized rods. To simulate a nonreflecting infinite plane wave, a perfectly matched layer is set at both ends of the simulated system [20]. The material and geometry parameters adopted in the numerical simulation (in dimensionless form) are $\rho_1 S_1 l_1/m = 15$, $\rho_2 S_{2l_2} l_2/m = 70$, $E_1 l_1/k = 6$, $E_2 l_2/k = 30$,

$S_1/l_1^2 = 0.01$, $S_{2l_2}/l_2^2 = 0.01$, $S_{2l_2}/S_{20} = 9$, $l_1/d = l_2/d = 50$, $\Gamma d^2/k = 5$, $\alpha = 1$, and the number of the units in the nonlinear mass-spring chain is 16. These parameters may not be optimal, but they are enough to verify the effectiveness of the proposed AD model.

It is worth noting that for the realization of an AD, the driving frequency ω must locate near the cutoff frequency of the nonlinear chain and the amplitude of the driving force should be appropriately chosen such that, when the driving force acts on one end of the device, ω should locate in the passband. When the driving force acts on the other end, ω must fall into the band gap. In other words, the AD effect can only be observed in a narrow frequency range with specific wave amplitude. It is also worth noting that, if a unit cell of the nonlinear periodic chain comprises N masses, there will be $2N$ frequency ranges that can be used for wave modulation, and the locations of these frequency ranges can also be changed by adjusting the parameter α. Some more interesting phenomena are discussed at the end of this paper.

C. Results

1. High forward transmission without changing frequencies

Here, we choose a particular value of the normalized frequency $\bar{\omega} = 2.237$ and the amplitude of the driving force is taken as $|f| = 0.175kd$. Figures 3(a) and 3(b) illustrate the snapshot of the deformed shapes of the system at time point $1.5\pi/\bar{\omega}$ when the driving force acts on the left side and the right side, respectively. These figures illustrate clearly that when the force acts on the left side, $\bar{\omega}$ falls into the passband and the wave propagates through the nonlinear chain [the line with symbols in Fig. 3(a)] in the form
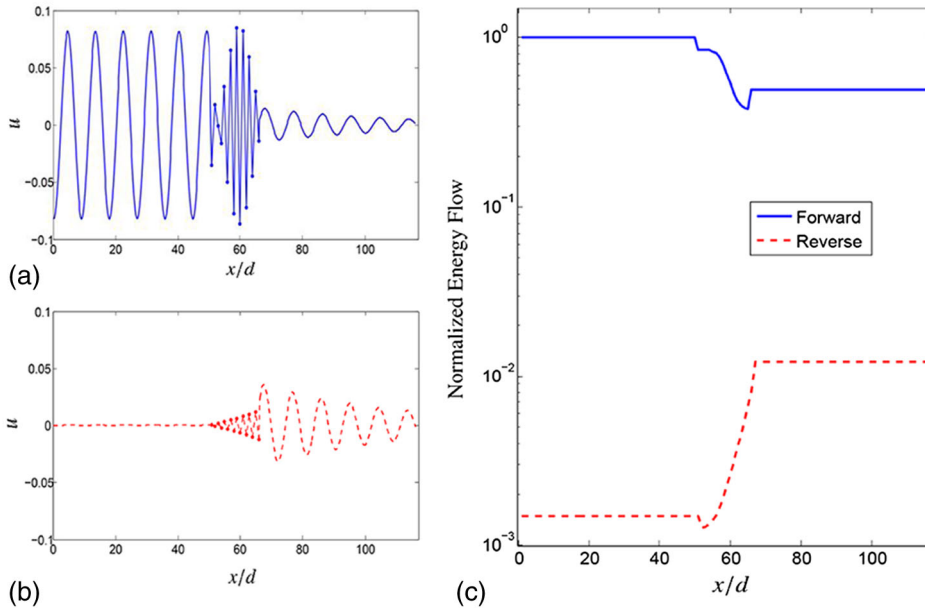
FIG. 3. A snapshot of the deformed shapes of the system at $t = 1.5\pi/\bar{\omega}$ when the driving force acts on the left side (a) and the right side (b). The lines with symbols denote the deformation of the nonlinear chain. (c) The spatial distributions of the time-averaged energy flux (or the internal power) as the acoustic wave is incident on the left side and the right side of the system.

of a Bloch wave. On the other hand, as the incident direction is reversed, $\bar{\omega}$ is in the band gap and the wave decays exponentially through the chain [the dashed line with symbols in Fig. 3(b)].

Figure 3(c) illustrates the spatial distribution of the time-averaged energy flux as the wave is incident from the left side and the right side of the system. The time-averaged energy flux is equal to the time-averaged energy-flux density multiplied by the cross-sectional area of the rod. In the nonlinear chain, the time-averaged energy-flux equals the time-average energy exchange between adjacent masses. The input power is not the same when the external force acts on the left side and right side. Actually, the input power is much larger when the wave comes from the left side. This indicates clearly that the response of the proposed AD is nonreciprocal, which is an important feature of true ADs, as pointed out in Ref. [18]. It is also worth noting that, although the wave-energy flux will decay when the wave goes through the structure from either direction, the underlying mechanism is quite different. The attenuation of the energy flux from the left side is caused by the mismatch of wave impedance at the interfaces between the nonlinear chain and rods. When the force acts at the right side, the wave is evanescent mainly because of multiple scatterings in the nonlinear chain rather than the impedance mismatch of the interfaces.

Even if the interface reflection is inevitable because of impedance mismatch, the power-transmission rate of the wave energy from the left side is still as high as $R_{Tl} = E_l^{\text{out}}/E_l^{\text{in}} \approx 0.5$. This value is much larger than those of other ADs in the literature [7,8,12]. It can be expected that the power-transmission rate can be even higher if the material properties and structures involved can be optimized appropriately, but it seems unlikely to reach the ideal value because of the difficulty in matching the impedances between the

discrete mass-spring chain and the continuous rods for this sample. Furthermore, the output powers associated with the left-side stimuli and right-side stimuli are $E_l^{\text{out}} \approx 3.4 \times 10^{-3}$ and $E_r^{\text{out}} \approx 1.0 \times 10^{-5}$, respectively. The former is almost 2 orders magnitude higher than the latter.

2. Forward, reverse, and breakdown characteristics

Figure 3 demonstrates the effectiveness of the present system as an AD, which restricts the energy flux in one particular direction and has a high forward-power-transmission rate. Because the transmission of the incident wave is amplitude dependent, it is necessary to analyze how the amplitude of the driving force will influence the output power of the acoustic wave. The output-energy flux W versus f is plotted in Fig. 4. The positive (negative) value of the force amplitude and the energy flux indicates that the wave comes from the left side (right side). It is clearly observed that the intrinsic relation between the force amplitude and the energy flux illustrated in Fig. 4 is very similar to the voltage-current-flow relationship of an electrical diode. Our AD also has the same forward, reverse, and breakdown characteristics as those known in an electrical diode. To be more specific, with a small forward bias, the frequency $\bar{\omega}$ is in the band gap of the nonlinear chain, where only a small normalized [divided by $E_1 S_1 d^2 \sqrt{k/(ml^2)}$] forward output power ($10^{-5}$–$10^{-6}$) is conducted. At a specific value of the forward force (i.e., $f \approx 0.17kd$), the diode starts to "conduct" significantly. This indicates that $\bar{\omega}$ has shifted to the passband and the mode of wave propagation in the nonlinear chain has also been changed. The force $f_d \approx 0.17kd$ can be called as the knee force or cut-in force as in the electrical diode. When the forward force is larger, the energy will propagate through the nonlinear chain in the form of a Bloch wave
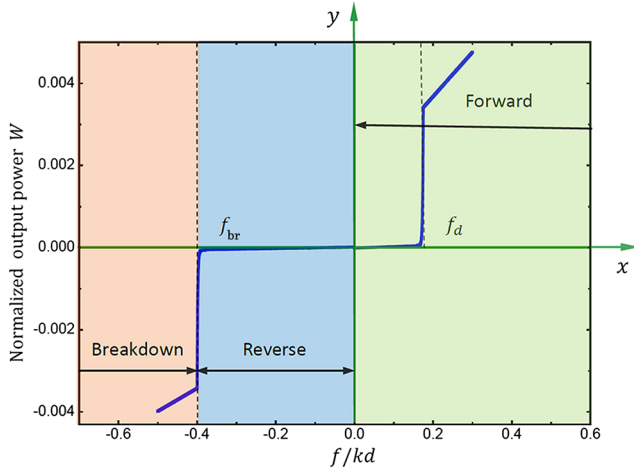
FIG. 4.   The output power W versus the driving force f. Note three main areas of operation: breakdown, reverse-biased, and forward-biased. Here, f_{br} and f_d denote the breakdown and conducting force, respectively. Both terms are borrowed from the electrical diode.

and the W-f curve will approach a straight line asymptotically because of the weak nonlinearity of the system. The reverse-biased situation is similar to the forward-biased one. When $-0.4kd < f \leq 0$, the AD has only a very small normalized reverse output power (10^{-7}–10^{-6}). While $f < -0.4kd$, a process called reverse breakdown occurs, which will lead to a large increase in the output power.

Therefore $f_{br} = -0.4kd$ can be called the breakdown force of the AD device. For an electrical diode, reverse breakdown usually damages the device permanently, but this is not the case for ADs. As shown in Fig. 4, when the magnitude of the force is larger than $|f_{br}|$, the wave can pass through the device from either direction. It is also obvious that the device can work as an AD when the amplitude of the external force is in the range of $[0.17kd, 0.40kd]$. A thermal diode with similar characteristics was proposed in Ref [22].

D. Further insight

Things will be more interesting if the nonlinear monatomic chain in the present AD model is replaced with a nonlinear polyatomic chain and the ratios of the masses in the unit cell can be chosen appropriately (the stiffness coefficients and the length of the springs are not changed).

The dispersion relationship of this nonlinear polyatomic chain can be calculated approximately through a perturbation approach [20] as

$$\bar{\omega} \approx \bar{\omega}_0 + \frac{3}{8}\frac{\Gamma d^2}{k}\frac{|\bar{A}_0|^2}{\bar{\omega}_0}, \tag{3}$$

where the linear dispersion with two branches can be obtained as

$$\bar{\omega}_0 = \frac{1}{2}\sqrt{2(2+\alpha)(1+\beta) \pm \sqrt{4(2+\alpha)^2(1+\beta)^2 - 16\beta(2+\alpha)^2 + 64\beta\cos^2(p)}}, \tag{4}$$

with $\beta = m_2/m_1$ denoting the masses ratio. Other parameters are the same as those adopted in the previous monatomic chain example.

The band diagram of the nonlinear diatomic chain with a masses ratio of $\beta = 1.01$ is illustrated in Fig. 5. In this case, the two branches of the dispersion are very close and they

are also amplitude dependent. As shown in Fig. 5(b), when the amplitude of the incident wave is small, the nondimensional frequency $\bar{\omega} = 1.75$ ($\bar{\omega} = \omega/\omega_1$, $\omega_1 = \sqrt{k/m_1}$) is in the optical branch (the upper branch) and therefore the incident wave can pass through the chain. When the amplitude is larger, the dispersion curves shift up so that
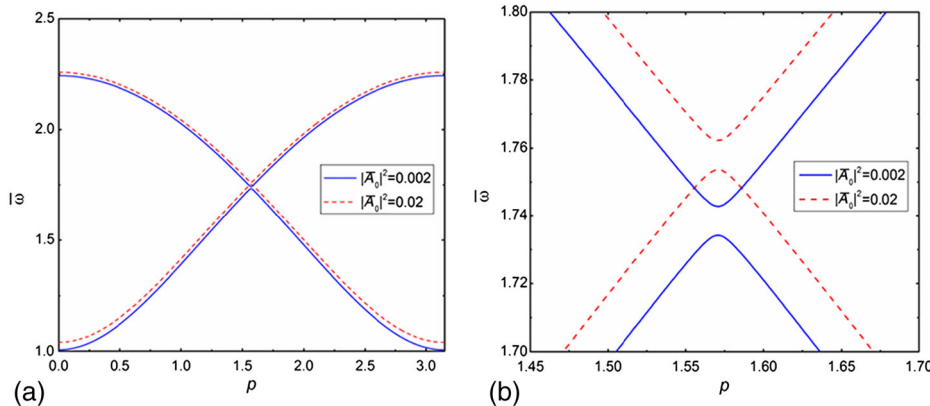

(a)

(b)

FIG. 5.   (a) The dispersion relationship of the nonlinear periodic diatomic chain with different amplitudes. Here, the masses ratio $\beta = 1.01$, and the spring parameters $\alpha = 1$, $\Gamma d^2/k = 5$ are the same as those in the previous monatomic chain. (b) A closer view of the dispersion behavior near the nondimensional frequency $\bar{\omega} = 1.75$.

$\bar{\omega} = 1.75$ will fall into the band gap and the wave cannot propagate through the chain. If the amplitude of the wave is increased further, the frequency $\bar{\omega} = 1.75$ will shift into the acoustic branch (the lower branch) of the passband and the wave can pass through again.

This phenomenon is similar to the tunneling effect in quantum mechanics. Consequently, it can be expected that if the nonlinear diatomic chain is used as the amplitude-dependent filter in an AD, the corresponding AD will have forward and reverse characteristics similar to the tunnel diode. The tunnel diode is also known as the Esaki diode, a special and important type of electricity diode. When a unit cell has more several masses, there will be much more operating-force ranges of the AD. To the best of our knowledge, there are still no similar diodes in electronics.

IV. DISCUSSION AND CONCLUSIONS

We present an AD model formed by coupling a weakly nonlinear periodic structure with asymmetric linear structures at two ends. Compared with other ADs in the literature, the proposed AD model can achieve wave rectification without changing the frequency of the incident wave and has a relatively high forward-power-transmission rate. We present numerical verification of a simple example of this model. A significant rectifying effect is observed at specific wave amplitudes and frequency ranges, and the forward-power-transmission rate of the AD is as high as 0.5. It can be expected that the power-transmission rate can be even higher if the material properties and structures can be optimized appropriately. Furthermore, the proposed AD model has very similar forward, reverse, and breakdown characteristics to those of electrical diodes.

The present model is sufficiently simple and efficient to encourage practical studies of experimental realization of this AD. The one-dimensional weakly nonlinear chain can be emulated by cross-combining the linear springs or one-dimensional array of granular crystals under precompression [12]. In fact, the asymmetric structural pattern can also be triggered by external forces [23,24] and, when the external forces are released, the induced structural asymmetry will disappear. This may provide the possibility of designing force-mediated, reversible, adaptive AD devices. Recent research also indicates that some materials can deform under the stimuli of external magnetic and electric fields. These mechanisms can be used to introduce a certain degree of tunability of the asymmetry of the linear structures in the present AD model. In this way, the band structure of the AD system can also be controlled actively by electric field, magnetic field, or prestress. In our future research, we will choose suitable materials and structures to do experiments and design more complex ADs whose operating-force ranges and efficiencies can be tuned by electric or magnetic fields and by prestress.

[1] F. D. M. Haldane and S. Raghu, Possible Realization of Directional Optical Waveguides in Photonic Crystals with Broken Time-Reversal Symmetry, Phys. Rev. Lett. **100,** 013904 (2008).

[2] Z. Wang, Y. D. Chong, J. D. Joannopoulos, and M. Soljačić, Reflection-Free One-Way Edge Modes in a Gyromagnetic Photonic Crystal, Phys. Rev. Lett. **100,** 013905 (2008).

[3] A. E. Serebryannikov, One-way diffraction effects in photonic crystal gratings made of isotropic materials, Phys. Rev. B **80,** 155117 (2009).

[4] B. Li, L. Wang, and G. Casati, Thermal Diode: Rectification of Heat Flux, Phys. Rev. Lett. **93,** 184301 (2004).

[5] B. Li, J. Lan, and L. Wang, Interface Thermal Resistance between Dissimilar Anharmonic Lattices, Phys. Rev. Lett. **95,** 104302 (2005).

[6] C. W. Chang, D. Okawa, A. Majumdar, and A. Zettl, Solid-state thermal rectifier, Science **314,** 1121 (2006).

[7] B. Liang, B. Yuan, and J. Cheng, Acoustic Diode: Rectification of Acoustic Energy Flux in One-Dimensional Systems, Phys. Rev. Lett. **103,**104301 (2009).

[8] B. Liang, X. S. Guo, J. Tu, D. Zhang, and J. C. Cheng, An acoustic rectifier, Nat. Mater. **9,** 989 (2010).

[9] S. Zhu, T. Dreyer, M. Liebler, R. Riedlinger, G. M. Preminger, and P. Zhong, Reduction of tissue injury in shock-wave lithotripsy by using an acoustic diode, Ultrasound Med. Biol. **30,** 675 (2004).

[10] S. A. Cummer, Selecting the direction of sound transmission, Science **343,** 495 (2014).

[11] L. Wang and B. Li, Thermal Logic Gates: Computation with Phonons, Phys. Rev. Lett. **99,** 177208 (2007).

[12] N. Boechler, G. Theocharis, and C. Daraio, Bifurcation-based acoustic switching and rectification, Nat. Mater. **10,** 665 (2011).

[13] X. F. Li, X. Ni, L. Feng, M. H. Lu, C. He, and Y. F. Chen, Tunable Unidirectional Sound Propagation through a Sonic-Crystal-Based Acoustic Diode, Phys. Rev. Lett. **106,** 084301 (2011).

[14] X. Zhu, X. Zou, B. Liang, and J. Cheng, One-way mode transmission in one-dimensional phononic crystal plates, J. Appl. Phys. **108,** 124909 (2010).

[15] Z. He, S. Peng, Y. Ye, Z. Dai, C. Qiu, M. Ke, and Z. Liu, Asymmetric acoustic gratings, Appl. Phys. Lett. **98,** 083505 (2011).

[16] S. Danworaphong, T. A. Kelf, O. Matsuda, M. Tomoda, Y. Tanaka, N. Nishiguchi, O. B. Wright, Y. Nishijima,

K. Ueno, S. Juodkazis, and H. Misawa, Real-time imaging of acoustic rectification, Appl. Phys. Lett. **99,** 201910 (2011).

[17] B. Yuan, B. Liang, J. Tao, X. Zou, and J. Cheng, Broadband directional acoustic waveguide with high efficiency, Appl. Phys. Lett. **101,** 043503 (2012).

[18] A. A. Maznev, A. G. Every, and O. B. Wright, Reciprocity in reflection and transmission: What is a "phonon diode"?, Wave Motion **50,** 776 (2013).

[19] R. Fleury, D. L. Sounas, C. F. Sieck, M. R. Haberman, and A. Alù, Sound isolation and giant linear nonreciprocity in a compact acoustic circulator, Science **343,** 516 (2014).

[20] R. K. Narisetti, M. J. Leamy, and M. Ruzzene, A perturbation approach for predicting wave propagation in one-dimensional nonlinear periodic structures, J. Vib. Acoust. **132,** 031001 (2010).

[21] A. Marathe and A. Chatterjee, Wave attenuation in nonlinear periodic structures using harmonic balance and multiple scales, J. Sound Vib. **289,** 871 (2006).

[22] K. I. Garcia-Garcia and J. Alvarez-Quintana, Thermal rectification assisted by lattice transitions, Int. J. Therm. Sci. **81,** 76 (2014).

[23] P. Wang, J. Shim, and K. Bertoldi, Effects of geometric and material nonlinearities on tunable band gaps and low-frequency directionality of phononic crystals, Phys. Rev. B **88,** 014304 (2013).

[24] S. H. Kang, S. Shan, A. Košmrlj, W. L. Noorduin, S. Shian, J. C. Weaver, D. R. Clarke, and K. Bertoldi, Complex Ordered Patterns in Mechanical Instability Induced Geometrically Frustrated Triangular Cellular Structures, Phys. Rev. Lett. **112,** 098701 (2014).